

Photoinduced Acceleration of the Effluent Rate of Developing Solvents in Azobenzene-Tethered Silica Gel

Masahiro Fujiwara,^{†,*} Minako Akiyama,[†] Momoko Hata,^{†,*} Kumi Shiokawa,[†] and Ryoki Nomura[‡]

[†]National Institute of Advanced Industrial Science and Technology, Kansai Center (Nanotechnology Research Institute), 1-8-31 Midorigaoka, Ikeda, Osaka 563-8577, Japan, and [‡]Department of Applied Chemistry, Osaka Institute of Technology, 5 Ohmiya, Asahi-ku, Osaka 535-8585, Japan

The control of molecular transfers is an important technique of modern science, because it is closely related to biological phenomena such as membrane transportation.¹⁻⁴ Some living bodies apply the solar or ATP energies to transport the ions and molecules, creating energies for life and controlling the cell environment.^{5,6} The manipulations of molecular transfers by artificial systems using light energy are also important research subjects of chemistry and photoscience.⁷⁻¹¹ The azobenzene moiety is one of the most familiar molecules that respond to light and is often applied to the photoresponsive material systems and devices.¹²⁻¹⁷ Especially, the switching of a molecular length of azobenzene between its trans and cis forms by photoisomerization originates various responsive stationary situations in the molecular level and/or nanolevel.¹⁸⁻²⁶ Some reports demonstrated that the photo-switching operations by the photoisomerization of azobenzene create macroscopic mechanical movements.^{18,19,22,23}

Molecular machine systems installed in ordered pore voids are currently active targets in the fabrication of functional nanomaterials.²⁷⁻³¹ As the diffusion behaviors (infiltration and defiltration) of molecules in nanopores are affected by the solid matrices, significantly different from bulk space, the substituents tethered on the mesoporous materials enable the domination of the molecular transports in these minute pore voids.³²⁻³⁷ These approaches revealed that the gating behaviors of the tethered substituents on mesoporous silicas control the accesses of molecules between the inside and outside of the mesopores.³⁸⁻⁵² Various kinds of stimuli and the corresponding responsive functional groups are employed for the gating

ABSTRACT The switching of a molecular length of azobenzene between its trans and cis forms by photoirradiation originates various photoresponsive systems in the molecular level and/or nanolevel. Recently, we and another group separately reported that some azobenzene-modified mesoporous silicas remarkably promote the release of molecules from the inside of the mesopore to the outside, when the lights, both UV and visible lights, were irradiated simultaneously. In these cases, the release rates of molecules were enhanced by the impeller-like effect of molecular motion of azobenzene moiety attributed to the continuous photoisomerization between the trans and cis isomers. This paper presents that azobenzene-substituent-tethered amorphous silica gel could promote the development of solvents in chromatography systems by photoirradiation. In column chromatography system where azobenzene-tethered silica gel was packed, the irradiation of both UV and visible lights increased the effluent rate of the developing solvents. The single irradiation of UV light scarcely enhanced the rate, while the visible light irradiation longer than 400 nm in wavelength also accelerated the development of the solvent moderately. The same kinds of phenomena were observed when this photopromoted chromatography system was applied to thin layer chromatography (TLC). Hydrocarbon developing solvents in the regions, where UV and visible lights were irradiated, moved up the TLC plate higher than those without photoirradiation. When the pyrene solution in the developing solvent was utilized in the chromatography systems, the similar photoacceleration of pyrene development was observed at the same level as the developing solvents.

KEYWORDS: amorphous silica · azobenzene · photoisomerization · column chromatography · photoacceleration

systems of mesoporous materials. Nowadays, these technologies are expected to be utilized in drug delivery and related applications.⁵³⁻⁵⁶ The good reversible performances of azobenzene photoisomerization are also used as promising photoresponsive gating systems of mesoporous materials.⁵⁷⁻⁶¹ The driving force of infiltration and defiltration produces the diffusion effect resulting from the concentration gradient of the molecules between the inside and outside of the mesopores in all the above-mentioned cases. The active acceleration of molecular release from mesopores by external stimulation will provide novel technologies of nanospace and molecules.^{6,8,62,63}

Recently we reported that the continuous photoisomerization of the azobenzene

*Address correspondence to m-fujiwara@aist.go.jp.

Received for review May 14, 2008 and accepted July 07, 2008.

Published online July 18, 2008. 10.1021/nn800290p CCC: \$40.75

© 2008 American Chemical Society

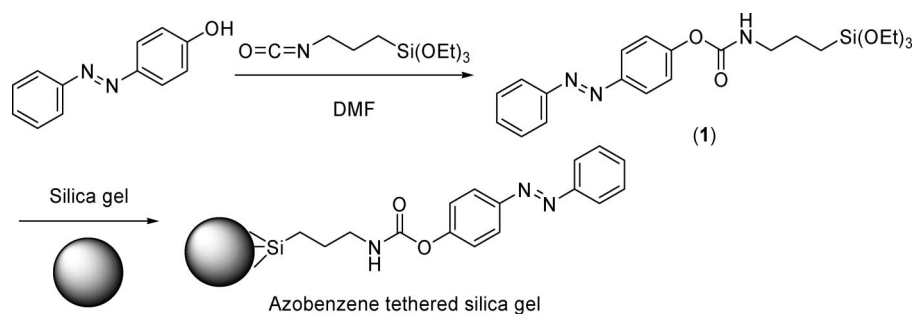


Figure 1. Preparation of azobenzene silane (compound **1**) and azobenzene-tethered silica gel.

group between its trans and cis forms, which is grafted on the surface of mesoporous silica, remarkably accelerates the release of cholesterol from the pore void.⁶⁴ The research groups of Prof. Zink and Prof. Stoddart also claimed analogous phenomena of the photodriven release system of azobenzene-tethered mesoporous silicas.^{65,66} Although the ordered pore structures of mesoporous materials must be advantageous to these photopromotion behaviors, the similar effects in less-ordered matrices will expand the versatility of these photoinduced technology systems. Moreover, the acceleration of the development of bulk solution by photoirradiation will be useful in microfluidic device systems. These considerations motivated us to attempt further applications of these photopromotions to the flow systems of solid matrices bearing less-ordered pore structures. In this paper, we report our latest researches on the photoinduced acceleration of molecular transports in chromatography systems using amorphous silica gel as a less-ordered solid matrix. When silica gels with a tethered azobenzene moiety were packed in common column chromatography and thin layer systems, the irradiations of light that cause the continuous photoisomerization of azobenzene moieties evidently increased the effluent rate of developing solvents and a monitor molecule.

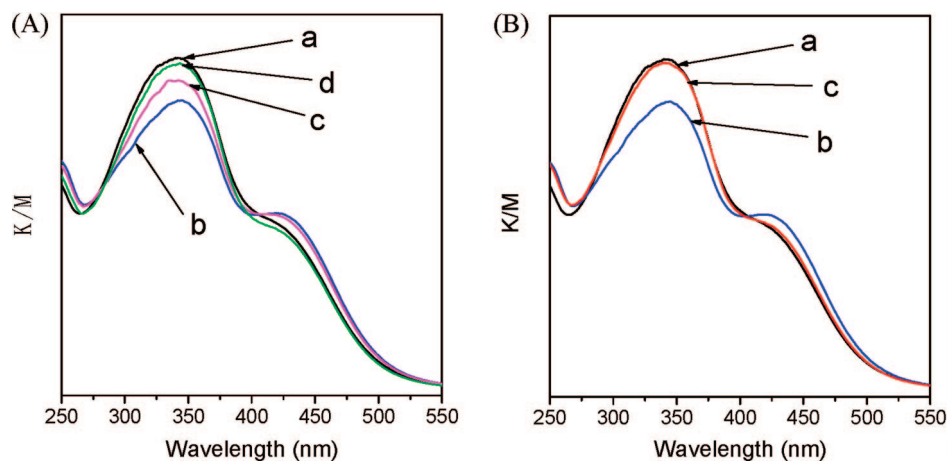


Figure 2. Diffuse reflectance UV-vis spectra of azobenzene-tethered silica gel under various irradiation conditions. Panel A: (a) without photoirradiation; (b) UV irradiation for 30 min; (c) 90 min in room light after UV irradiation for 30 min; (d) visible light irradiation for 20 min after UV irradiation for 30 min. Panel B: (a) without photoirradiation; (b) UV irradiation for 30 min; (c) UV and visible lights irradiation for 30 min.

RESULTS AND DISCUSSION

(1) Properties of Azobenzene-Tethered Silica Gel Particle. An azobenzene moiety was installed on the surface of a common silica gel by a grafting process as shown in Figure 1. The successful grafting of the azobenzene substituent was ensured by the orange color and the UV-vis spectrum of the silica gel solid. We also prepared *n*-octadecyl group-tethered silica

gel as a reference sample by the analogous procedures. The diffuse reflectance UV-vis spectrum of azobenzene-tethered silica gel is shown as line a in Figure 2A. Two characteristic absorptions of azobenzene moiety at 340 and 430 nm were clearly found in this azobenzene-tethered silica gel. These absorptions are naturally absent in the original (not modified) silica gel and the *n*-octadecyl-group-tethered one. Figure 3A indicates the nitrogen adsorption-desorption isotherms of the original silica gel and azobenzene-tethered silica gel. The original silica gel had a broad peak of mesopores around 7 nm in diameter according to the BJH pore distribution plot. The specific surface area and the pore volume of this silica gel were calculated to be 544 m²/g or 0.703 mL/g, respectively, as listed in Table 1. The nitrogen sorption isotherm of the azobenzene-tethered silica gel was slightly changed from the original ones, and the corresponding specific surface area and the pore volume decreased approximately 10% from the original silica gel (to 492 m²/g and 0.637 mL/g, respectively). On the other hand, the peak pore diameter was the same as before grafting as shown in the pore size distribution of Figure 3C. The nitrogen adsorption-desorption isotherm of *n*-octadecyl group-tethered silica gel was also compared with that of the original silica gel (Figure 3B). The changes of isotherms,

specific surface area, and pore volume were approximately similar to the azobenzene-tethered silica gel. Therefore, the pore structures of these two modified silica gels are thought to be analogous. *n*-Octadecyl triethoxysilane molecule is slightly longer than the compound **1** according to the molecular sizes calculated by Chem 3D (shown in the Supporting Information). As the pore size of the original silica gel is large enough, no significant differences of the pore structures were observed in the difference of these substituents. It should be noted that

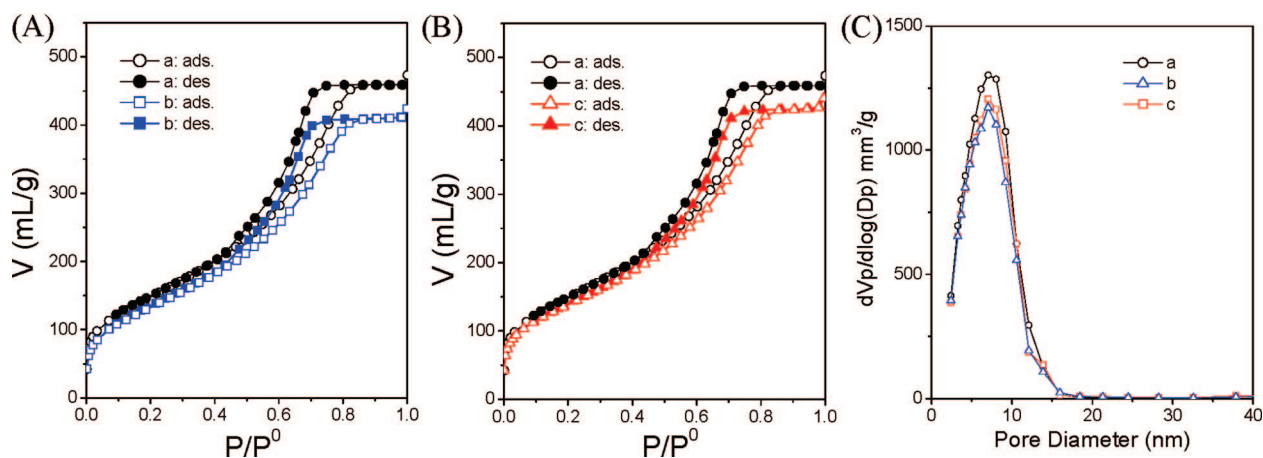


Figure 3. Panel A: Nitrogen adsorption–desorption isotherms of (a) the original silica gel and (b) azobenzene-tethered silica gel. Panel B: Nitrogen adsorption–desorption isotherms of (a) the original silica gel and (c) *n*-octadecyl-tethered silica gel. Panel C: BJH pore size distributions using the adsorption branches of the corresponding isotherms.

these modified silica gel materials still had wide pores (approximately 7 nm) in comparison with the hydrocarbons we employed as developing solvents in this research.

The changes of UV–vis spectra by the photoirradiation are also shown in Figure 2A and 2B. The irradiation of UV light (approximately from 310 to 400 nm in wavelength) using band-pass filter U350 and an average glass filter caused the photoisomerization from trans to cis isomer. Under these conditions, the reverse isomerization from cis to trans isomer was not favorable. After the UV irradiation for 30 min, the absorption around 340 nm decreased and that around 430 nm increased considerably as shown in line b of Figure 2A. This change of UV–vis spectrum is a typical observation that trans azobenzene isomerizes to the cis isomer. Thus, the photoisomerization occurred smoothly even in the case of azobenzene-tethered on the surface of silica gel. Although the reverse isomerization of cis to trans isomer occurs by heat as well as visible light, this isomerization proceeded very slowly at room temperature in darkish room light. Even after 90 min after the UV irradiation was stopped, the returns of the UV–vis absorptions at 340 and 430 nm were moderate as shown in line c of Figure 2A. However, the visible light irradiation longer than approximately 410 nm for 20 min smoothly regenerated the trans isomer (line d in Figure 2A). Therefore, the irradiation of the visible light was necessary for the rapid reverse isomerization of the azobenzene moiety. When both UV and visible lights from 310 to 800 nm in wavelength were irradiated, the decrease of the absorption around 340 nm and the in-

crease around 430 nm were stopped after 30 min with slight variations (line c in Figure 2B). Even when the irradiation time was extended for over 120 min, no further change of the UV–vis spectrum was observed to indicate that the photoisomerization achieved an equilibrium situation. In this case, it is thought that the azobenzene moiety-tethered silica gel sample isomerized between trans and cis isomers continuously.

(2) Photopromotion of Effluent Rate of Developing Solvent in Column Chromatography. This azobenzene-tethered silica gel was packed in a range of 3.5 cm long into a Pyrex glass tube for column chromatography. Various kinds of lights were irradiated to this packed silica gel using the experiment arrangement shown in Figure 4. At first, the effluent rates of developing solvents without photoirradiation (in darkish room light) were monitored as standard times for draining of a certain volume of solvents. The promotion effects of the various photoirradiations on the effluent rate (time) were indicated with enhanced ratios compared with the standard times without photoirradiation. The results of these promotion effects are summarized in Table 2.

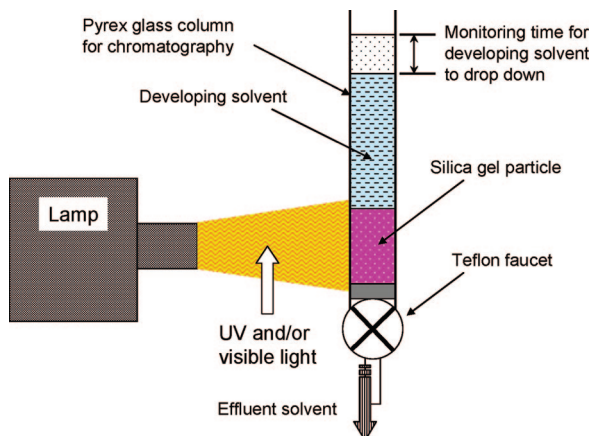


Figure 4. The pattern diagram of the experimental arrangement for light-promoted development of solvent in column chromatography.

TABLE 1. Porosity Data of Various Silica Gel Samples

sample	SSA (m ² /g) ^a	PPD (nm) ^b	PV (mL/g) ^c
original silica gel	543.56	7.05	0.7027
azobenzene-tethered	492.43	7.05	0.6366
octadecyl-tethered	507.70	7.05	0.6585

^aSpecific surface area calculated by BET method. ^bPeak pore diameter estimated by BJH method. ^cPore volume estimated by BJH method.

TABLE 2. Promoted Effects of Various Photoirradiations on Effluent Rates of Developing Solvents^a

sample	developing solvent	effluent time (sec)	wavelength of irradiated light (nm)			
			310–800	310–400	400–800	500–800
no tethered	decahydronaphthalene	320	±0	±0	±0	±0
	tetradecane	318	±0	±0	±0	±0
	decane	196	+1	±0	±0	±0
azobenzene	decahydronaphthalene	450	+13	±0	+11	+7
	tetradecane	470	+13	±0	+12	+7
	decane	468	+9	±0	+8	+6
octadecyl	decahydronaphthalene	470	+1	±0	+1	+1
	tetradecane	401	±0	±0	±0	±0
	decane	390	±0	±0	±0	±0

^aPromotion effect is calculated from [(time for effluent without photoirradiation/time for effluent with photoirradiation) – 1] × 100.

When no tethered silica gel (original silica gel) was used, no promotions on the effluent rates of developing solvents were observed in all kinds of the photoirradiations. Although the common silica gel absorbs no irradiated lights, a slight increase of the temperature (approximately from 2 to 5 °C) was detected during the photoirradiation. Although the temperature elevation might decrease the viscosity of solvents to promote their development in silica gel, a negligible increase of the effluent rate was found only in the case of decane solvent. Furthermore, when a heating cut filter (HA50) was not used, the temperature elevation sometimes reached about 12 °C. However, no significant differences of the effluent rates were detected between with and without the heating cut filter. Thus, the influences of the temperature increase and the resulting viscosity decrease on the effluent rate could be excluded in our research system. On the other hand, the promotion effect of some photoirradiations was remarkably found in the cases of azobenzene-tethered silica gel as summarized in Table 2. For example, the effluent rate was enhanced about 13% with UV and visible lights irradiation compared with no irradiation, when decahydronaphthalene was used as eluent developing solvent. In all solvents employed in this research (decahydronaphthalene, tetradecane, decane), the increases of the effluent rates were observed clearly. The promotion effect in the case of decane was lower than decahydronaphthalene and tetradecane, suggesting that the molecular sizes of developing solvents might be involved in this promotion effect. Even the irradiations of visible lights with longer wavelength than 400 or 500 nm increased the effluent rate as well as the simultaneous irradiation of UV and visible lights, although the acceleration effects were lower. It is reported that this visible light irradiation enhances the release rate of molecules from azobenzene-tethered mesoporous silica by the continuous photoisomerization of the azobenzene group between trans and cis isomers.^{65,66} However, the most effective enhancement of the effluent rates was found in the case of the irradiation of both UV and visible lights, where the continu-

ous isomerization of azobenzene between the trans and cis isomer is accelerated more efficiently.

It is noteworthy that the irradiation of single UV light from 310 to 400 nm in wavelength had no promotion effect on the effluent rate of the developing solvents. In our previous report about the release behaviors of cholesterol from M41s-type mesoporous silica, although the promotion effect by UV light was less than simultaneous UV and visible lights, the release rate was higher than the single visible light irradiation and no photoirradiation.⁶⁴ It was also reported that the isomerization of azobenzene from the trans to cis isomer promotes the access of molecules in the pore voids of ordered mesoporous materials.^{58,59} In these reported cases, the photoisomerization from trans to cis isomer shortens the molecular length of azobenzene substituents, expanding the effective pore size of the channels. Consequently, the expansion of the effective pore size reduces the obstruction effect of the azobenzene substituents to result in the improvement of the accesses of molecules in the mesopores.^{58,59} In the meantime, in our present case with amorphous silica gel the shortening of the molecular length of the azobenzene substituents might have no significant effects on the diffusion of molecules in the irregular and interconnected pore structures. As mentioned before, the peak pore diameter of the azobenzene-tethered silica gel was measured to be 7.05 nm, which was sufficiently wide compared with the shortened molecular length of azobenzene moiety by the isomerization (approximately 0.34 nm).⁵⁸ It is considered that the extension of the effective pore size was not responsible for the obvious acceleration effect on the effluent rate found in the cases of azobenzene-tethered silica gel with UV and visible irradiation (and only visible light irradiation). This promotion effect must be caused by the continuous and repetitive isomerization of the azobenzene moiety tethered on the silica gel surface between the trans and cis forms in a similar fashion to our previous case and other reports.^{64–66}

The same types of experiments were carried out using octadecyl-group-tethered silica gel. The molecular length of this substituent is comparable with the

azobenzene substituent we employed here. Although octadecyl group scarcely absorbs UV and visible lights, molecular movements of this linear long alkyl chain tethered on the surface of silica gel might bring some enhancement effects on the effluent rate. However, no promotion effects were observed in all the cases of octadecyl-group-tethered silica gel as listed in Table 2. Thus, it was concluded that the increases of the effluent rate of the aliphatic hydrocarbon solvents in the azobenzene-tethered silica gel under suitable photoirradiation conditions were caused by the expulsion effect of the continual propylal movement of azobenzene moiety. As a summary, the repeated motion of azobenzene moiety that was tethered on silica gel surface enhanced the development of some aliphatic solvents in column chromatography system. The release of molecules from the inside to the outside of mesopores has already been accelerated in the reported cases.^{64–66} In the present case, the photopromotion of fluid development was also achieved using the movement of azobenzene.

(3) Photopromotion of Effluent Rate of Developing Solvent in Thin Layer Chromatography. In the previous paragraph, the photoirradiation that induces the continuous motion of the azobenzene moiety between the trans and cis isomers increased the effluent rates of aliphatic development solvents in column chromatography system. This phenomenon could be also applied to a thin-layer-type of chromatography system. On a ready-made silica gel TLC plate, the same solution of the compound **1** used for the preparation of the azobenzene-tethered silica gel particle was pasted in approximately 5 cm height. The azobenzene-tethered TLC plate thus obtained was set in a common TLC developing chamber as shown in Figure 5. To the central part of this azobenzene-modified part, various kinds of lights were irradiated during a hydrocarbon solvent is developing. The size of the main irradiated circular area was approximately 5 cm in diameter. After the developing solvent attained a certain level sufficiently higher than the azobenzene-tethered area, the developed height levels of the solvent were compared between the regions with and without the photoirradiation.

Figure 6 illustrates some picture images of silica gel TLC plates used for these experiments, where decahydronaphthalene was employed as developing solvent. In the case of original silica gel TLC plate (without tethered azobenzene), the borderline of the developed solvent was horizontally straight even when UV and visible lights were irradiated. No bulgy parts of the borderline were found in all areas including the photoirradiated region (Figure 6A). Without photoirradiation, no flexion of the borderline of the developed solvent was observed in the azobenzene-tethered silica gel TLC plate (Figure 6B). When UV

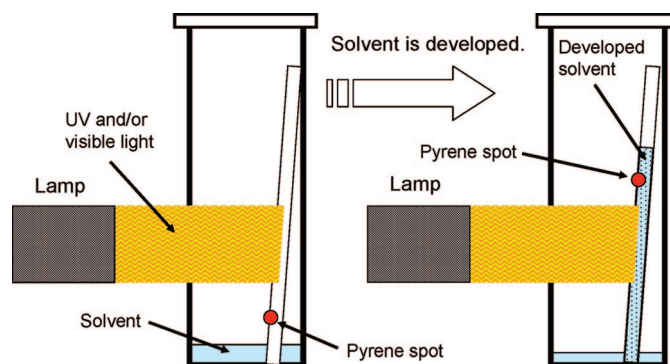


Figure 5. The pattern diagram of the experimental arrangement for photopromoted solvent development in TLC experiment system.

and visible lights were simultaneously irradiated to the azobenzene-modified area of the TLC plate, the central part of the borderline was clearly raised upward as shown in Figure 6C. The difference of the distances from the button to the borderline between the central part and the left side was approximately 7 mm. This observation indicated that the exposure of the central region of the azobenzene-modified silica gel thin layer TLC to UV and visible lights accelerated the development rate of the solvent to curve the borderline upward. However, the single UV irradiation to the same place as the UV and visible lights resulted in no convex borderline of the developing solvent (Figure 6D). As ob-

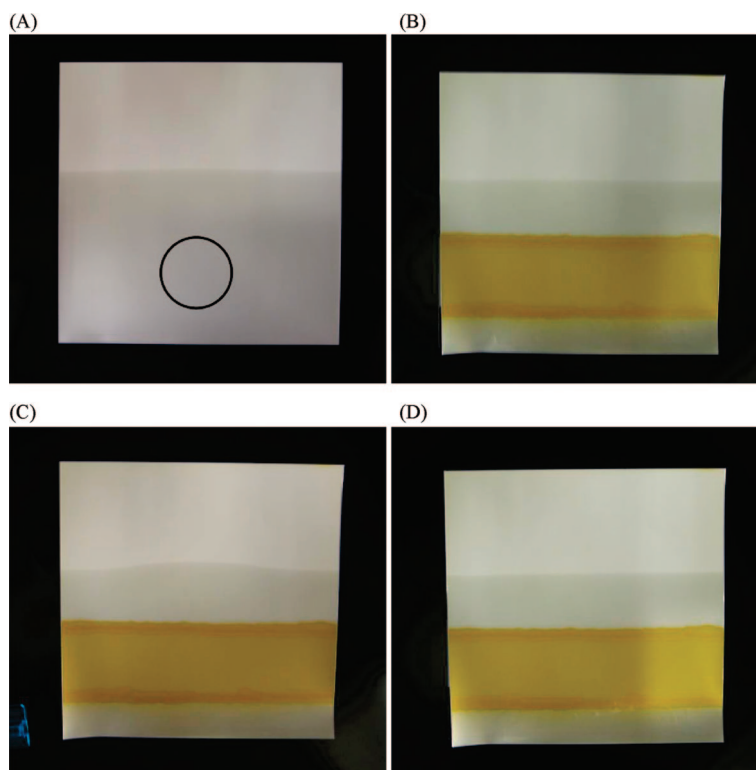


Figure 6. Pictures of silica gel TLC plate used for solvent developing experiments. (A) No-tethered (original) TLC plate with UV and visible light irradiation. The main region, where UV and visible lights were irradiated, was indicated with black circle. In experiments C and D, the respective lights were irradiated at the approximately same areas as this TLC plate: (B) azobenzene-tethered TLC plate without photoirradiation (in darkish room light); (C) azobenzene-tethered TLC plate with UV and visible light irradiation; (D) azobenzene-tethered TLC plate with UV light irradiation.

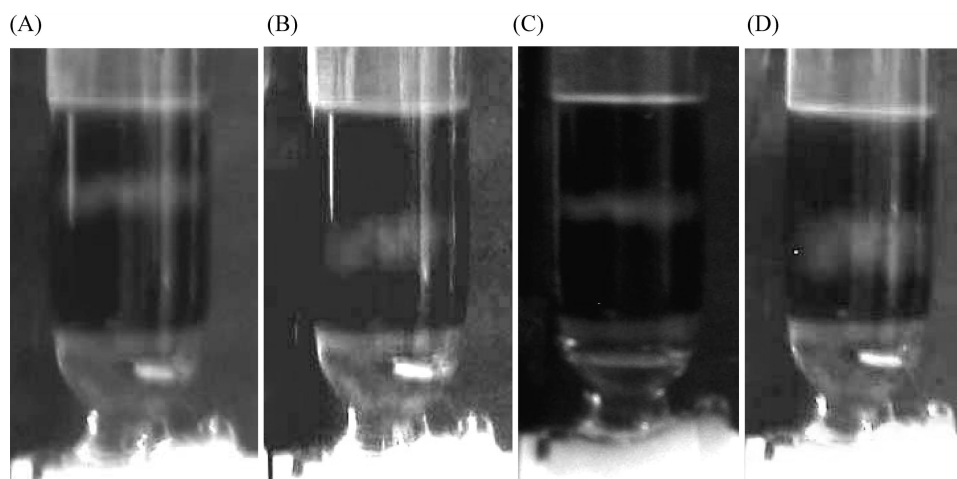


Figure 7. The pictures of fluorescent observation of pyrene in azobenzene-tethered silica gel in column chromatography under various photoirradiation conditions. The lights were irradiated from the left-hand: (A, B) with the irradiation of UV and visible lights; (C) without photoirradiation; (D) with the irradiation of UV light.

served above, the formation of the convex borderline induced by the acceleration of the development rate of the solvent took place only when the UV and visible lights were simultaneously irradiated to the azobenzene-tethered region of the TLC plate. These results are consistent with those of the column chromatography mentioned in the previous section. Consequently, the photoacceleration of the effluent rate of the developing solvents in azobenzene-tethered silica gel was observed even in the thin layer chromatography system.

(4) Fluorescent Analysis of the Photopromotion of the Effluent Rate in Azobenzene-Tethered Silica Gel. Previous papers reported that the release of molecules inside the ordered mesopores of silica materials to the bulk solution phase is promoted by the continuous reversible motion of the azobenzene moiety.^{64–66} The transportation of some monitor molecules from the mesopores to the solutions was analyzed in these cases, while the diffusion rate of the solvents was not measured. Our present research revealed that the effluent rate of developing solvents in amorphous silica gel was accelerated by the repeated movement of the azobenzene moiety tethered on the silica surface. This meant that the spreading of solvent molecules (not monitor molecules) was enhanced by the photoirradiation. Then, we examined the effect of the photoirradiation on the transportation of a larger monitor molecule dissolving in the developing solvents. These approaches are also expected to ascertain the detailed mechanism of the accelerated release of monitor molecules from the pore voids of mesoporous materials. There are two possibilities of the mechanism of the release promotion of monitor molecules. The first possibility is that the movement of the azobenzene moiety directly accelerates the transportation of the monitor molecules. The second one is that the movement increases the diffusion of the solvent molecule to result in enhancing the spreading of

the monitor molecules as well. For these experiments, we selected pyrene as a monitor molecule, because this molecule is a relatively large molecule and fluorescent which will be advantageous for clear observation of its developing behaviors.

At first, pyrene was loaded at the top of the stationary phase of a silica gel particle using decahydronaphthalene solution in the similar manner to the separation procedure of column chromatography. The acceleration effect of the irradiation of UV and visible lights on the effluent

rate of decahydronaphthalene was ensured even in the case of the pyrene solution, when azobenzene-tethered silica gel was used (results are not shown here). The regions of pyrene were monitored using its fluorescent emission at appropriate times during the development of the pyrene–decahydronaphthalene solution. We also found that the effluence of pyrene with simultaneous UV and visible light irradiation was faster than that with other irradiations, no light irradiation, and single UV irradiation. Figure 7 shows the fluorescent observation pictures of pyrene in azobenzene-tethered silica gel of column chromatography under various irradiation conditions. These four images of fluorescent pyrene were captured with excitation light emission during a temporary halt of the photoirradiation. Figure 7 panels A and B are pictures of the fluorescent pyrene at different times, when UV and visible light were irradiated from the left-hand. The luminous white domains where pyrene existed were inclined toward the left side clearly. The inclination of the luminous domains of pyrene became steeper with its descent (Figure 7B). These observations meant that the effluent rate of the left side was higher than the right side. It is thought that the irradiated light from the left-hand activated azobenzene moieties in the left part more efficiently than those in the right part, resulting in higher effluent of the molecules in the left side. On the other hand, the domains where pyrene located looked horizontal in the both cases of no photoirradiation (Figure 7C) and single UV irradiation to azobenzene-tethered silica gel (Figure 7D).

Then, we examined the detail relations between the effluent rates of developing solvent and pyrene. The fractions of the drained developing solutions were collected every 3 min or every 1.3 mL in separate experiments. In these experiments, decane was employed as developing solvent, because the effluent rate was comparatively high to be suitable for

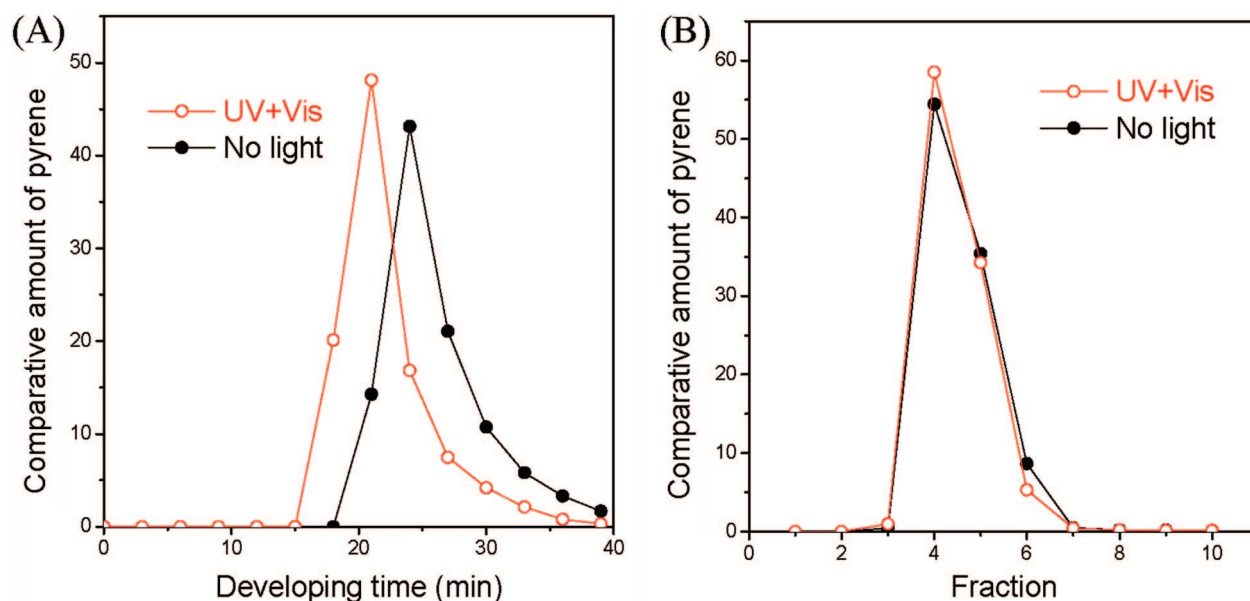


Figure 8. The comparison of the pyrene contents in the respective fractions of decane solutions drained from azobenzene-tethered silica gel column. The comparative amounts of pyrene were estimated by capillary GC analysis: (A) as a function of developing time (3 min); (B) as a function of fraction (1.3 mL).

collecting the constant amount of the eluent solvent. Figure 8 shows the pyrene contents in the respective fractions of the drained decane solutions as functions of developing time (Figure 8A) or fraction number (Figure 8B). The vertical axes indicate the relative amounts of pyrene determined by the peak areas of GC analysis in each fraction. As can be seen in Figure 8A, it was ascertained that the pyrene effluent rate was enhanced by the simultaneous irradiation of UV and visible lights in comparison to no photoirradiation. The maximum of pyrene effluence with the UV and visible light irradiation was observed at the fraction from 21 to 24 min, whereas the maximal content of pyrene was detected in the fraction from 24 to 27 min in the case of no photoirradiation. The variations of the pyrene contents as a function of fraction number are illustrated in Figure 8B. The times required for filling up each fraction with drained decane to ensure the promotion effects of the photoirradiations in these cases are summarized in Table 3. The results in Table 3 demonstrated that the effluent rate was certainly enhanced with the UV and visible light irradiation. If the photopromotion of the effluent rate of pyrene is mainly caused by the direct interaction between the pyrene and azobenzene moiety, there must be some differences between the effluent rates of pyrene and decane solvent. However, the two plots with UV-visible lights and without photoirradiation in Figure 8B completely overlapped to indicate that the developments of pyrene and decane were equally enhanced by the photoirradiation. Therefore, it is likely that the increase of the effluent rate of pyrene

was principally caused by the accelerated developing of decane by the UV and visible light irradiation.

The promotion of pyrene development was also found in the case of silica gel TLC. The two images in left-hand side (top and bottom) of Figure 9 are the pictures of the same TLC plate after a pyrene solution in decahydronaphthalene was developed in the original (no tethered azobenzene) TLC plate with the simultaneous UV and visible light irradiation. The picture A (top) was photographed in room light, and the picture C (bottom) was in the dark with UV excitation light. The photoirradiation area was similar to the cases of the TLC experiment mentioned previously. Although some deposition of pyrene species on silica gel was found (dark-colored regions in the central area of the picture A), both the borderline of the developed decahydronaphthalene (Figure 9A) and the developed pyrene spots (Figure 9C) were horizontal. On the other hand, in the same TLC experiment using azobenzene-tethered silica gel, the central regions of the white pyrene spots observed in Figure 9D appeared higher than other regions as well as the borderline of the developed decahydronaphthalene (Figure 9B).

From these observations, the photopromotion of pyrene effluence must be caused by the indirect effect of the photoinduced motion of the azobenzene moiety

TABLE 3. Times (in Minutes) Required for Filling up Each Fraction in Figure 8B

Fraction	1	2	3	4	5	6	7	8	9	10
UV + vis	2.22	4.45	7.07	9.26	11.49	14.09	16.78	18.47	21.09	23.30
no light	2.35	5.12	7.48	10.22	12.58	15.34	18.11	20.47	23.22	25.57

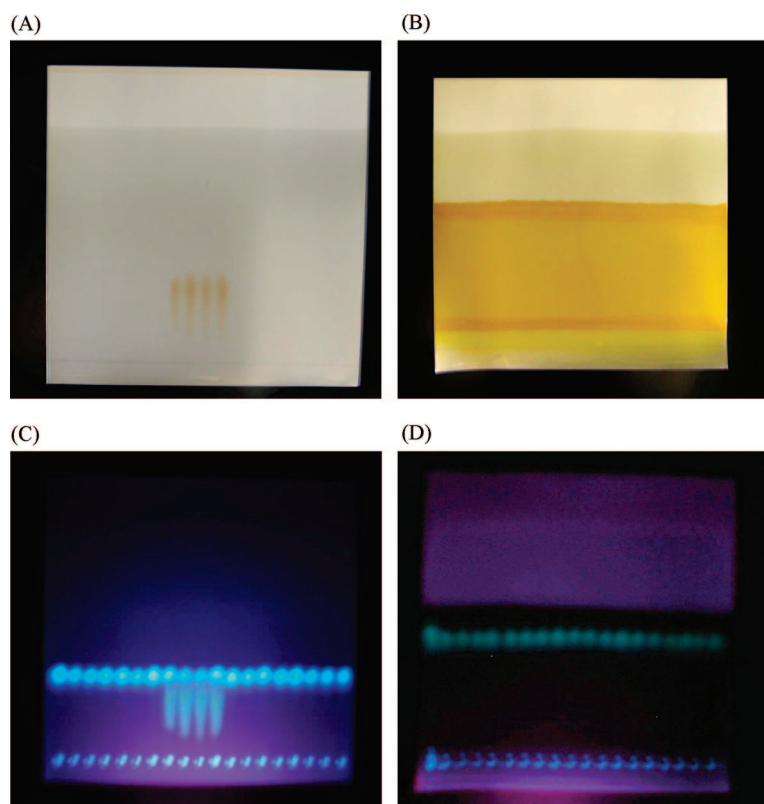


Figure 9. Images of developments of pyrene solution in decahydronaphthalene in a TLC system with simultaneous UV and visible light irradiation: (A) image of original (no tethered azobenzene) TLC plate in room light; (B) image of azobenzene-tethered TLC plate in room light; (C) image of original (no tethered azobenzene) TLC plate in dark with UV excitation light; (D) image of azobenzene-tethered TLC plate in dark with UV excitation light.

through the coexisting solvent. Although this chromatography system cannot be regarded as the same as the previously reported cases of the photoaccelerated releases of molecules from the mesopore materials,^{64–66} the influences of coexisting solvents on the effluent rate of monitor molecules from the mesopores are essential to the photopromoted release reported.

EXPERIMENTAL SECTION

Chemicals. 4-Hydroxyazobenzene (4-phenylazophenol), 3-(triethoxysilyl)propyl isocyanate, octadecyltriethoxysilane, pyrene and other chemicals such as decahydronaphthalene (as mixture of trans and cis isomers) employed here were commercially available ones, and used without further purification. Dry solvents utilized in this study were purchased as dried solvents and used without further treatment. Amorphous silica gel we utilized in this research was Merck Silica gel 60 for column chromatography. The thin layer chromatography plate of silica gel was also purchased from Merck (TLC aluminum sheet 20 cm × 20 cm Silica gel 60).

Preparation of Azobenzene-Tethered Silica Gel Particle. 4-(3-Triethoxysilylpropylaminocarbonyloxy)azobenzene (compound **1**) was prepared by the direct reaction of 4-hydroxyazobenzene (1.08 g, 5.433 mmol) and 3-(triethoxysilyl)propyl isocyanate (1.33 g, 5.377 mmol) in dry DMF at 120 °C for 24 h as shown in Figure 1. The complete consumption of the isocyanate was ensured by the disappearance of a characteristic infrared absorption of the isocyanate at 2271 cm⁻¹. This DMF solution was directly

CONCLUSIONS

This paper revealed that the continuous movement of azobenzene moiety tethered on the surface of amorphous silica gel between its trans and cis forms by some photoirradiations remarkably increased the effluent rates of developing solvents in chromatography systems. The single irradiation of UV light was not effective to accelerate the rate. The photoirradiations to isomerize azobenzene moiety not only from the trans to cis isomer but also from the cis to trans one, such as the simultaneous irradiation of UV and visible lights, were essential to this photopromotion. The movement of the azobenzene group increases the fluidity of molecules inside the pores of silica gel, enhancing the effluent rate of developing solvents and coexisting molecules. The focus of the applications of the photoresponsive properties of azobenzene groups have been on the switching functions of the photoisomerization between its trans and cis forms, but the effects of the continuous motion have not received attention in recent times. However, the accelerations of molecular transports using photoirradiation are potent novel technologies in the manipulation of molecules with various photo-techniques. Moreover, the accelerations of molecular transports using lights will provide a new technology in the conversion of photoenergy into other forms such as motional energy. These kinds of technologies are closely related to photovoltaic generation. Although the acceleration of molecular transportations reported here was not active transport, our results provide the control systems of the spreading of molecules at the nano level. The acceleration of the effluent of solvents by the photoisomerization of the azobenzene moiety we reported here might be applied to microfluid device systems as well.

used for grafting on amorphous silica gel. Silica gel particles (Merck Silica gel 60) were dried at 150 °C for 2 h prior to grafting. The DMF solution of compound **1** (5 ml) was added to the dry toluene (125 mL) with suspension of 15.00 g of the dried silica gel. This mixture was refluxed for about 18 h, and the volatiles were removed under reduced pressure. The orange color solid thus obtained was heated at 80 °C in air for 20 h to form the tight binding of azobenzene substituent with silica surface. This solid was washed with acetone (800 mL to 15 g of the solid) two times, and finally dried at 70 °C for 6 h. Octadecyl group-tethered silica gel was obtained by the analogous procedures using octadecyltriethoxysilane instead of the compound **1**.

Measurement Procedure of the Effluent Rate of the Developing Solvent in Column Chromatography. The azobenzene-tethered silica gel was packed in a range of about 3.5 cm long as stationary phase into column chromatography tube made of Pyrex glass (1.5 cm in inner diameter) with the bottom of the glass filter (filter size: G-2). At the upper part of the outlet, a faucet made of Teflon was located to control the effluent. This system was totally analogous to the common column chromatography for separation. Eluent

developing solvents are filled on the top of the silica gel. To this packed silica gel, various kinds of lights were irradiated from one side using Xenon short arc lamp (USHIO UXL-500SX) with USHIO OPTICAL Module X. The distance from the irradiation cylinder to the column was about 5 cm. When the distance between the irradiation cylinder and the column was increased, the promotion effect on the effluent rate was diminished probably because of the decrease of the illuminance of the irradiation light. Therefore, the experimental arrangement shown in Figure 4 was strictly fixed and was never moved during research. The pattern diagram of this experimental arrangement is shown in Figure 4. In all experiments, both an average glass filter to remove UV light shorter than about 310 nm in wavelength and a heating cut filter (HA50) to absorb infrared light longer than approximately 690 nm in wavelength were set in the front of the lamp. Thus, neither short-wavelength UV light nor infrared light was irradiated to the silica gel. Strong UV light might cause some decompositions of the substituent, and the infrared light might produce some considerable heat effects on this experiment. These influences should be eliminated for revealing the propelling effects of the continuous photoisomerizations of azobenzene. The additional filters to regulate the wavelength ranges of irradiation lights were fixed at 1 cm from the column. A filter U350 was for UV light transmission, L42 and Y52 were for visible light transmission obtained from HOYA Corporation. The light transmission characteristics of these filters are shown in Supporting Information.

In all experiments of the solvent developing, only aliphatic hydrocarbons that absorbed neither UV light nor visible light used for the irradiation were employed as developing solvents. The Teflon faucet of the column was fully opened during the experiment. The times required for the dropping down of developing solvents in a certain level were monitored visually from three to five times (depending on repeatability), and the average times are adopted as experimental results. The reproducibility of the effluent times was generally high (within $\pm 5\%$). The certain levels of the dropped developing solvents were varied from 0.5 to 6 cm depending on the effluent periods of the solvents. The times needed for the dropping were fixed in the range of from 3 to 8 min. The initial height of the developing solvents was fixed in all cases, because the volume (and the weight) of the solvents located in the upper part of the silica gel might influence the effluent rate of the solvents. The promotion effects of the photoirradiation listed in Table 2 are estimated by the following calculations. Actual volumes and times for the effluent are summarized in Supporting Information. These values indicated the enhanced effluent rates compared with the standard times obtained in the experiments without photoirradiation. When no change of the effluent rate was observed, the promotion effect is calculated to be 0 (zero).

$$\text{promotion effect} = (T_0 / T_1 - 1) \times 100$$

where T_0 and T_1 are times for the effluent without photoirradiation or with photoirradiation, respectively.

The procedures of the experiments using pyrene as a fluorescent monitor molecule was approximately the similar manner to the separation technique using column chromatography without the sea sand of the top of the silica gel stationary phase. A 0.2 mL portion of the concentrated pyrene (nearly saturated) solution of the effluent solvent was pipetted on the top of the silica gel. The position of developed pyrene with the eluent solvent was monitored as a luminous band with the aid of a common UV lamp with temporary blocking of the photoirradiation. The contents of pyrene in sampled fraction solutions were analyzed by a capillary GC apparatus (Shimadzu GC-1800).

Preparation of Azobenzene-Tethered Silica Gel Thin Layer. Azobenzene moiety was installed on a silica gel thin layer plate by a grafting procedure. At first, 5 mL of the solution of the compound **1** obtained in the previous section was dissolved in 15 mL of dry toluene. This impregnation solution was infiltrated into the silica gel of Merck thin layer plate (20 cm \times 20 cm) to the entire width of the plate between 3 and 8 cm from the button of the plate. The entire solution was impregnated uniformly to the above domain. This plate was heated at 160 °C for 12 h in air to

remove the volatiles and to form stable bonds between the organic substituent and silica surface. The plate thus obtained was immersed in 1 L of acetone two times for washing and finally dried at room temperature over 24 h.

Measurement Procedure of the Effluent Rate of the Developing Solvent in Thin Layer Chromatography. This procedure was essentially similar to the common TLC chromatography except for the photoirradiation. A thin layer plate obtained by the aforementioned procedures was dipped into a developing solvent in a glass container, and the container was sealed with a glass plate cover. The center part of the azobenzene-tethered silica gel thin layer was exposed to various kinds of lights from a Xenon short arc lamp previously mentioned. The distance from the irradiation cylinder to the plate was approximately 5 cm. When the solvent reached approximately 7–8 cm from the top side of the plate, the plate was taken out from the container, and the distance of the boundary of the solvent from the bottom was immediately measured. The pictures of TLC plates were taken by a common digital camera. The experimental technique of pyrene developing was also analogous to the thin layer chromatography manipulation. Approximately 19 small spots of the solution containing pyrene (in the same solvent as developing solvent) were applied to a plate about 1.5 cm from the bottom. Then, this plate was dipped in the container, and the various kinds of lights were irradiated in the same manners as described above. The regions of developed pyrene were monitored as luminous spots with the aid of the handy UV lamp.

Analyses. SEM (scanning electron microscopy) images were measured using a JEOL JSM-6390 scanning electron microscope apparatus. Infrared spectra were monitored with a Perkin-Elmer Spectrum One spectrometer. Diffuse reflectance UV spectra were obtained with a JASCO V-550 spectrometer equipped with an integrating sphere. Kubelka–Munk functions were plotted against the wavelength. Nitrogen adsorption–desorption isotherms were obtained at -196 °C (in liquid N_2) using a Bellsorp Mini instrument (BEL JAPAN, Inc.). Outgassing was performed under dry nitrogen flow at 100 °C over 12 h. BET plots were used for estimating the specific surface area of the silica samples. BJH calculations were applied to evaluate the mesopore sizes and the pore volumes using adsorption branches of the isotherms.

Acknowledgment. The authors acknowledge the support of the Fuji Film Company for this research.

Supporting Information Available: Actual average times of drained developing solvents, SEM images of silica samples, molecular structures of the silane compounds; color forms of Figure 2 to enhance understanding, and the transmittance characteristics of various light filters. This material is available free of charge via the Internet at <http://pubs.acs.org>.

REFERENCES AND NOTES

- Klingenberg, M. Membrane Protein Oligomeric Structure and Transport Function. *Nature* **1981**, *290*, 449–454.
- Gruenberg, J.; Maxfield, F. R. Membrane Transport in the Endocytic Pathway. *Curr. Opin. Cell Biol.* **1995**, *7*, 552–563.
- Ikonen, E. Roles of Lipid Rafts in Membrane Transport. *Curr. Opin. Cell Biol.* **2001**, *13*, 470–477.
- Boxer, S. G. Molecular Transport and Organization in Supported Lipid Membranes. *Curr. Opin. Cell Biol.* **2000**, *4*, 704–709.
- Sweadner, K. J.; Goldin, S. M. Active Transport of Sodium and Potassium Ions: Mechanism, Function, and Regulation. *New Engl. J. Med.* **1980**, *302*, 777–783.
- Kyte, J. Molecular Considerations Relevant to the Mechanism of Active Transport. *Nature* **1981**, *292*, 201–204.
- Lewis, N. S. Light Work with Water. *Nature* **2001**, *414*, 589–590.
- Gust, D.; Moore, T. A.; Moore, A. L. Mimicking Photosynthetic Solar Energy Transduction. *Acc. Chem. Res.* **2001**, *34*, 40–48.
- Bennett, I. M.; Vanegas Farfano, H. M.; Bogani, F.; Primak, A.; Liddell, P. A.; Otero, L.; Sereno, L.; Silber, J. J.; Moore,

- A. L.; Moore, T. A.; Gust, D. Active Transport of Ca^{2+} by an Artificial Photosynthetic Membrane. *Nature* **2002**, *420*, 398–401.
10. Steinberg-Yfrach, G.; Rigaud, J.-L.; Durantini, E. N.; Moore, A. L.; Gust, D.; Moore, T. A. Light-Driven Production of ATP Catalysed by FOF1-ATP Synthase in an Artificial Photosynthetic Membrane. *Nature* **1998**, *392*, 479–482.
 11. Steinberg-Yfrach, G.; Liddell, P. A.; Hung, S.-C.; Moore, A. L.; Gust, D.; Moore, T. A. Conversion of Light Energy to Proton Potential in Liposomes by Artificial Photosynthetic Reaction Centres. *Nature* **1997**, *385*, 239–241.
 12. Kumar, G. S.; Neckers, D. C. Photochemistry of Azobenzene-Containing Polymers. *Chem. Rev.* **1989**, *89*, 1915–1925.
 13. Ichimura, K. Photoalignment of Liquid-Crystal Systems. *Chem. Rev.* **2000**, *100*, 1847–1873.
 14. Xie, S.; Natansohn, A.; Rochon, P. Recent Developments in Aromatic Azo Polymers Research. *Chem. Mater.* **1993**, *5*, 403–411.
 15. Anzai, J. I.; Osa, T. Photosensitive Artificial Membranes Based on Azobenzene and Spirobenzopyran Derivatives. *Tetrahedron* **1994**, *50*, 4039–4070.
 16. Ikeda, T.; Tsutsumi, O. Optical Switching and Image Storage by Means of Azobenzene Liquid-Crystal Films. *Science* **1995**, *268*, 1873–1875.
 17. Norikane, Y.; Tamaoki, N. Light-Driven Molecular Hinge: A New Molecular Machine Showing a Light-Intensity-Dependent Photoresponse that Utilizes the Trans-Cis Isomerization of Azobenzene. *Org. Lett.* **2004**, *6*, 2595–2598.
 18. Barrett, C. J.; Mamiya, J. I.; Yager, K. G.; Ikeda, T. Photo-Mechanical Effects in Azobenzene-Containing Soft Materials. *Soft Matter* **2007**, *3*, 1249–1261.
 19. Jiang, H.; Kelch, S.; Lendlein, A. Polymers Move in Response to Light. *Adv. Mater.* **2006**, *18*, 1471–1475.
 20. Seki, T. Dynamic Photoresponsive Functions in Organized Layer Systems Comprised of Azobenzene-Containing Polymers. *Polym. J.* **2004**, *36*, 435–454.
 21. Katsonis, N.; Lubomska, M.; Pollard, M. M.; Feringa, B. L.; Rudolf, P. Synthetic Light-Activated Molecular Switches and Motors on Surfaces. *Prog. Surf. Sci.* **2007**, *82*, 407–434.
 22. Ichimura, K.; Oh, S.-K.; Nakagawa, M. Light-Driven Motion of Liquids on a Photoresponsive Surface. *Science* **2000**, *288*, 1624–1626.
 23. Yu, Y.; Nakano, M.; Ikeda, T. Photomechanics Directed Bending of a Polymer Film by Light. *Nature* **2003**, *425*, 145.
 24. Shibaev, V.; Bobrovsky, A.; Boiko, N. Photoactive Liquid Crystalline Polymer Systems with Light-Controllable Structure and Optical Properties. *Prog. Polym. Sci.* **2003**, *28*, 729–836.
 25. Sakai, H.; Orihara, Y.; Kodashima, H.; Matsumura, A.; Ohkubo, T.; Tsuchiya, K.; Abe, M. Photoinduced Reversible Change of Fluid Viscosity. *J. Am. Chem. Soc.* **2005**, *127*, 13454–13455.
 26. Renner, C.; Moroder, L. Azobenzene as Conformational Switch in Model Peptides. *ChemBioChem* **2006**, *7*, 869–878.
 27. Stein, A.; Melde, B. J.; Schroden, R. C. Hybrid Inorganic-Organic Mesoporous Silicates - Nanoscopic Reactors Coming of Age. *Adv. Mater.* **2000**, *12*, 1403–1419.
 28. Sayari, A.; Hamoudi, S. Periodic Mesoporous Silica-Based Organic-Inorganic Nanocomposite Materials. *Chem. Mater.* **2001**, *13*, 3151–3168.
 29. Stein, A. Advances in Microporous and Mesoporous Solids - Highlights of Recent Progress. *Adv. Mater.* **2003**, *15*, 763–775.
 30. Hoffmann, F.; Cornelius, M.; Morell, J.; Froba, M. Silica-Based Mesoporous Organic-Inorganic Hybrid Materials. *Angew. Chem., Int. Ed.* **2006**, *45*, 3216–3251.
 31. Wan, Y.; Zhao, D. Y. On the Controllable Soft-Templating Approach to Mesoporous Silicates. *Chem. Rev.* **2007**, *107*, 2821–2860.
 32. Eijkel, J. C. T.; van den Berg, A. Water in Micro- and Nanofluidics Systems Described using the Water Potential. *Lab Chip* **2005**, *5*, 1202–1209.
 33. Todd, B. D. Cats, Maps and Nanoflows: Some Recent Developments in Nonequilibrium Nanofluidics. *Mol. Simul.* **2005**, *31*, 411–428.
 34. Sansom, M. S. P.; Biggin, P. C. Biophysics Water at the Nanoscale. *Nature* **2001**, *414*, 156–159.
 35. Majumder, M.; Chopra, N.; Andrews, R.; Hinds, B. J. Nanoscale Hydrodynamics Enhanced Flow in Carbon Nanotubes. *Nature* **2005**, *438*, 44.
 36. Wasan, D. T.; Nikolov, A. D. Spreading of Nanofluids on Solids. *Nature* **2003**, *423*, 156–159.
 37. Walcarius, A.; Etienne, M.; Lebeau, B. Rate of Access to the Binding Sites in Organically Modified Silicates. 2. Ordered Mesoporous Silicas Grafted with Amine or Thiol Groups. *Chem. Mater.* **2003**, *15*, 2161–2173.
 38. Vallet-Regi, M.; Ramila, A.; del Real, R. P.; Perez-Pariente, J. A New Property of MCM-41: Drug Delivery System. *Chem. Mater.* **2001**, *13*, 308–311.
 39. Munoz, B.; Rimila, A.; Pérez-Pariente, J.; Diaz, I.; Vallet-Regi, M. MCM-41 Organic Modification as Drug Delivery Rate Regulator. *Chem. Mater.* **2003**, *15*, 500–503.
 40. Mal, N. K.; Fujiwara, M.; Tanaka, Y. Photocontrolled Reversible Release of Guest Molecules from Coumarin-Modified Mesoporous Silica. *Nature* **2003**, *421*, 350–353.
 41. Mal, N. K.; Fujiwara, M.; Tanaka, Y.; Taguchi, T.; Matsukata, M. Photo-Switched Storage and Release of Guest Molecules in the Pore Void of Coumarin-Modified MCM-41. *Chem. Mater.* **2003**, *15*, 3385–3394.
 42. Fu, Q.; Rao, G. V. R.; Ista, L. K.; Wu, Y.; Andrzejewski, B. P.; Sklar, L. A.; Ward, T. L.; López, G. P. Control of Molecular Transport through Stimuli-Responsive Ordered Mesoporous Materials. *Adv. Mater.* **2003**, *15*, 1262–1266.
 43. Hernandez, R.; Tseng, H.-R.; Wong, J. W.; Stoddart, J. F.; Zink, J. I. An Operational Supramolecular Nanovalve. *J. Am. Chem. Soc.* **2004**, *126*, 3370–3371.
 44. Casasús, R.; Marcos, M. D.; Martínez-Máñez, R.; Ros-Lis, J. V.; Soto, J.; Villaescusa, L. A.; Amorós, P.; Beltrán, D.; Guillem, C.; Latorre, J. Toward the Development of Ionically Controlled Nanoscopic Molecular Gates. *J. Am. Chem. Soc.* **2004**, *126*, 8612–8613.
 45. Nguyen, T. D.; Tseng, H.-R.; Celestre, P. C.; Flood, A. H.; Liu, Y.; Stoddart, J. F.; Zink, J. I. A Reversible Molecular Valve. *Proc. Natl. Acad. Sci. U.S.A.* **2005**, *102*, 10029–10034.
 46. Fujiwara, M.; Terashima, S.; Endo, Y.; Shiokawa, K.; Ohue, H. Switching Catalytic Reaction Conducted in Pore Void of Mesoporous Material by Redox Gate Control. *Chem. Commun.* **2006**, 4635–4637.
 47. Aznar, E.; Casasús, R.; García-Acosta, B.; Marcos, M. D.; Martínez-Máñez, R.; Sancenón, F.; Soto, J.; Amorós, P. Photochemical and Chemical Two-Channel Control of Functional Nanogated Hybrid Architectures. *Adv. Mater.* **2007**, *19*, 2228–2231.
 48. Cheng, K.; Landry, C. C. Diffusion-Based Deprotection in Mesoporous Materials: A Strategy for Differential Functionalization of Porous Silica Particles. *J. Am. Chem. Soc.* **2007**, *129*, 9674–9684.
 49. Nguyen, T. D.; Leung, K. C.-F.; Liong, M.; Liu, Y.; Stoddart, J. F.; Zink, J. I. Versatile Supramolecular Nanovalves Reconfigured for Light Activation. *Adv. Funct. Mater.* **2007**, *17*, 2101–2110.
 50. Nguyen, T. D.; Liu, Y.; Saha, S.; Leung, K. C.-F.; Stoddart, J. F.; Zink, J. I. Design and Optimization of Molecular Nanovalves Based on Redox-Switchable Bistable Rotaxanes. *J. Am. Chem. Soc.* **2007**, *129*, 626–634.
 51. Zhua, Y.; Shi, J. A Mesoporous Core-Shell Structure for pH-Controlled Storage and Release of Water-Soluble Drug. *Microporous Mesoporous Mater.* **2007**, *103*, 243–249.
 52. Park, C.; Oh, K.; Lee, S. C.; Kim, C. Controlled Release of Guest Molecules from Mesoporous Silica Particles Based on a pH-Responsive Polypseudorotaxane Motif. *Angew. Chem., Int. Ed.* **2007**, *46*, 1455–1457.
 53. Vallet-Regi, M.; Balas, F.; Arcos, D. Mesoporous Materials for Drug Delivery. *Angew. Chem., Int. Ed.* **2007**, *46*, 7548–7558.

54. Trewyn, B. G.; Slowing, I. I.; Giri, S.; Chen, H. T.; Lin, V. S. Y. Synthesis and Functionalization of a Mesoporous Silica Nanoparticle Based on the Sol–Gel Process and Applications in Controlled Release. *Acc. Chem. Res.* **2007**, *40*, 846–853.
55. Trewyn, B. G.; Giri, S.; Slowing, I. I.; Lin, V. S. Y. Mesoporous Silica Nanoparticle Based Controlled Release, Drug Delivery, and Biosensor Systems. *Chem. Commun.* **2007**, 3236–3245.
56. Ariga, K.; Vinu, A.; Hill, J. P.; Mori, T. Coordination Chemistry and Supramolecular Chemistry in Mesoporous Nanospace. *Coord. Chem. Rev.* **2007**, *251*, 2562–2591.
57. Weh, K.; Noack, M.; Hoffmann, K.; Schroder, K.-P.; Caro, J. Change of Gas Permeation by Photoinduced Switching of Zeolite-Azobenzene Membranes of Type MFI and FAU. *Microporous Mesoporous Mater.* **2002**, *54*, 15–26.
58. Liu, N. G.; Chen, Z.; Dunphy, D. R.; Jiang, Y. B.; Assink, R. A.; Brinker, C. J. Photoresponsive Nanocomposite Formed by Self-Assembly of an Azobenzene-Modified Silane. *Angew. Chem., Int. Ed.* **2003**, *42*, 1731–1734.
59. Liu, N. G.; Dunphy, D. R.; Atanassov, P.; Bunge, S. D.; Chen, Z.; Lopez, G. P.; Boyle, T. J.; Brinker, C. J. Photoregulation of Mass Transport through a Photoresponsive Azobenzene-Modified Nanoporous Membrane. *Nano Lett.* **2004**, *4*, 551–554.
60. Maeda, K.; Nishiyama, T.; Yamazaki, T.; Suzuki, T.; Seki, T. Reversible Photoswitching Liquid-Phase Adsorption on Azobenzene Derivative-Grafted Mesoporous Silica. *Chem. Lett.* **2006**, *35*, 736–737.
61. Tanaka, T.; Ogino, H.; Iwamoto, M. Photochange in Pore Diameters of Azobenzene-Planted Mesoporous Silica Materials. *Langmuir* **2007**, *23*, 11417–11420.
62. Zhang, E. Y.; Phelps, M. A.; Cheng, C.; Ekins, S.; Swaan, P. W. Modeling of Active Transport Systems. *Adv. Drug Delivery Rev.* **2002**, *54*, 329–354.
63. Gokel, G. W.; Carasel, I. A. Biologically Active, Synthetic Ion Transporters. *Chem. Soc. Rev.* **2007**, *36*, 378–389.
64. Zhu, Y. C.; Fujiwara, M. Installing Dynamic Molecular Photomechanics in Mesopores: A Multifunctional Controlled-Release Nanosystem. *Angew. Chem., Int. Ed.* **2007**, *46*, 2241–2244.
65. Angelos, S.; Choi, E.; Vogtle, F.; De Cola, L.; Zink, J. I. Photo-Driven Expulsion of Molecules from Mesostructured Silica Nanoparticles. *J. Phys. Chem. C* **2007**, *111*, 6589–6592.
66. Angelos, S.; Johansson, E.; Stoddart, J. F.; Zink, J. I. Mesostructured Silica Supports for Functional Materials and Molecular Machines. *Adv. Funct. Mater.* **2007**, *17*, 2261–2271.